

Meranti—three of which struck during September alone. Several other Saffir–Simpson category 3 and 4 intensity level systems during 2016 had major impacts: (1) Hurricane Nicole in the North Atlantic; (2) Typhoons Chaba, Haima, Malakas, Megi, Lionrock, Nepartik, and Nock-Ten in the western North Pacific; and (3) Typhoon Victor in the Southwest Pacific. Also noteworthy was that 2015/16 was the first year since the onset of the satellite era in 1970 that no major HTC’s were observed in the Australian basin.

2) ATLANTIC BASIN—G. D. Bell, E. S. Blake, C. W. Landsea, C. Wang, J. Schemm, T. Kimberlain, R. J. Pasch, and S. B. Goldenberg

(i) Seasonal activity

The 2016 Atlantic hurricane season produced 15 named storms, of which 7 became hurricanes and 4 became major hurricanes (Fig. 4.21a). The HURDAT2 30-year (1981–2010) seasonal averages (as embodied in IBTrACS) are 11.8 tropical (named) storms, 6.4 hurricanes, and 2.7 major hurricanes (Landsea and Franklin 2013).

The 2016 seasonal ACE value (Bell et al. 2000) was about 148% of the 1981–2010 median ($92.4 \times 10^4 \text{ kt}^2$;

Fig. 4.21b), which is above NOAA’s lower threshold (120% of the median) for an above-normal season (see www.cpc.ncep.noaa.gov/products/outlooks). Based on this ACE value, combined with above-average numbers of named storms, hurricanes, and major hurricanes, NOAA officially classified the 2016 Atlantic hurricane season as above normal. This was the first above-normal season since 2012, producing more than 2.5 times the average ACE value of the last three seasons 2013–15.

(ii) Storm tracks and landfalls

The Atlantic hurricane main development region (MDR; green boxed region in (Fig. 4.22a) spans the tropical Atlantic Ocean and Caribbean Sea between 9.5° and 21.5°N (Goldenberg and Shapiro 1996; Goldenberg et al. 2001; Bell and Chelliah 2006). A main delineator between more- and less-active Atlantic hurricane seasons is the number of hurricanes and major hurricanes that first become named storms within the MDR during the peak months (August–October; ASO) of the hurricane season.

During ASO 2016, eight named storms formed in the MDR (Fig. 4.20), with five becoming hurricanes and four of those becoming major hurricanes. Three hurricanes were observed over the Caribbean Sea, a region with only one hurricane during the past three seasons (2013–15). The MDR activity during 2016 is comparable to the above-normal season averages for the MDR of 8.2 named storms, 6.0 hurricanes, and 3.0 major hurricanes. In contrast, the MDR averages for the last three seasons were 5.0 named storms with 2.3 becoming hurricanes and 1.0 becoming a major hurricane. These values are near the MDR averages for seasons that are not classified as above normal: 3.3 named storms, 2.0 hurricanes, and 1.0 major hurricanes.

Another feature of the 2016 season was that two major hurricanes (Matthew and Nicole) formed during October and accounted for more than 50% of the seasonal ACE value. The October 2016 ACE value was more than 50% larger than that of any other October since at least 1981 (Schreck et al. 2014).

The 2016 Atlantic hurricane season included a sharp increase in the number of landfalling storms compared to the last three seasons. In the United States, five named storms made landfall, including two hurricanes: Tropical Storm Bonnie and Hurricane Matthew struck South Carolina; Tropical Storms Colin and Julia, and Hurricane Hermine made landfall in Florida. This was the most U.S. landfalling storms since 2008 (six storms). Hermine was not only the first landfalling hurricane in the United

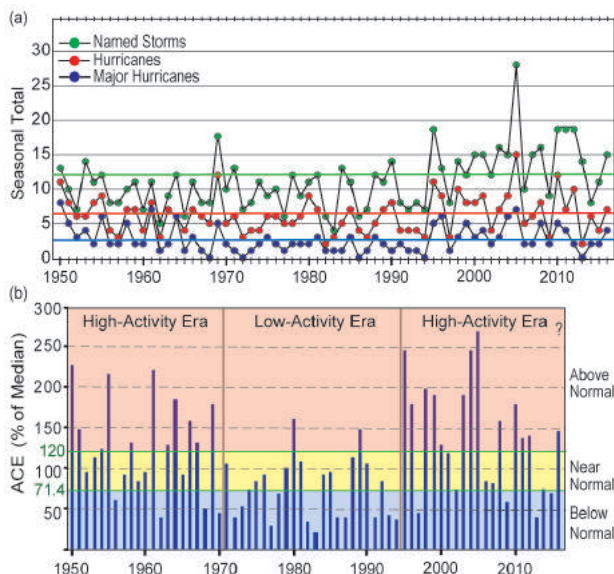


FIG. 4.21. Seasonal Atlantic hurricane activity during 1950–2016. (a) Numbers of named storms (green), hurricanes (red), and major hurricanes (blue), with 1981–2010 seasonal means shown by solid colored lines. (b) ACE index expressed as percent of the 1981–2010 median value. ACE is calculated by summing the squares of the 6-hourly maximum sustained surface wind speed (knots) for all periods while the storm is at least tropical storm strength. Red, yellow, and blue shadings correspond to NOAA’s classifications for above-, near-, and below-normal seasons, respectively. Vertical brown lines separate high- and low-activity eras. High and low activity eras are defined per Goldenberg et al. (2001).

States since 2014, but also the first hurricane to make landfall in Florida since Hurricane Wilma in 2005.

Several storms during 2016 also made landfall outside of the United States. The most significant of these was major Hurricane Matthew, which reached maximum sustained surface wind speeds of 140 kt (72 m s^{-1}) over the Caribbean Sea and remained at major hurricane status for eight days (30 Septem-

ber–7 October). Matthew made landfall as a category 4 storm in Haiti, Cuba, and the Bahamas, causing extensive damage and loss of life in all three countries, before making landfall in South Carolina as a category 1 hurricane. Matthew is discussed further in Sidebar 4.1. Other landfalling storms included Tropical Storm Danielle in Mexico, Hurricane Earl in Belize, and Hurricane Otto in Nicaragua.

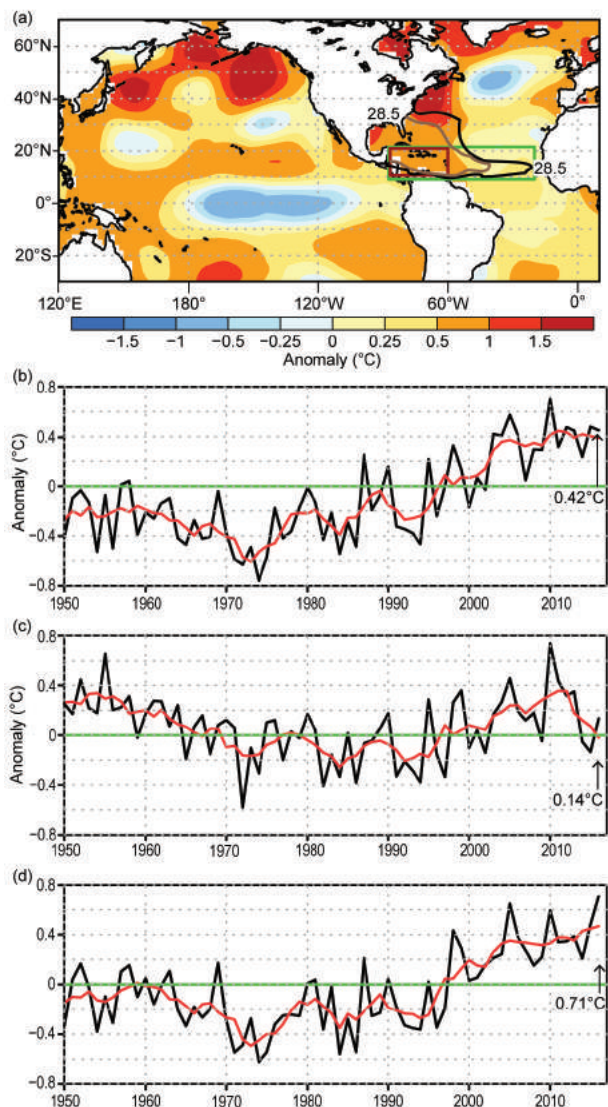


FIG. 4.22. (a) ASO 2016 SST anomalies ($^{\circ}\text{C}$), with the observed (black contours) and climatological (brown contours) 28.5°C SST isotherms shown. (b) 1950–2016 of ASO area-averaged SST anomalies ($^{\circ}\text{C}$) in the MDR [green box in (a)]. (c) Difference between ASO area-averaged SST anomalies ($^{\circ}\text{C}$) in the MDR and those for the entire global tropics (20°N – 20°S). (d) ASO area-averaged SST anomalies ($^{\circ}\text{C}$) in the Caribbean Sea [red box in (a)] spanning 60° – 87.5°W and 10° – 21.5°N . Red lines in (b)–(d) show a 5-pt. running mean of each time series. Anomalies are departures from the ERSST-v4 (Huang et al. 2015) 1981–2010 monthly means.

(iii) Atlantic sea surface temperatures

Within the MDR, SST anomalies during ASO 2016 (Fig. 4.22a) were $+0.45^{\circ}\text{C}$ above the 1981–2010 average (Fig. 4.22b), and they were also warmer ($+0.14^{\circ}\text{C}$ warmer) than the average departure for the global tropics (Fig. 4.22c). Over the Caribbean Sea, SSTs were $+0.71^{\circ}\text{C}$ above average, which is the highest value in the 1950–2016 record (Fig. 4.22d).

The warm phase of the Atlantic multidecadal oscillation (AMO; Enfield and Mestas-Nuñez 1999) and the associated positive phase of the Atlantic meridional mode (Vimont and Kossin 2007; Kossin and Vimont 2007) are the primary climate factors associated with high-activity eras for Atlantic hurricanes (Goldenberg et al. 2001; Bell and Chelliah 2006; Bell et al. 2011, 2012). This warm phase features anomalously high SSTs in the MDR compared to the remainder of the global tropics, as can be seen during the high-activity era of 1950–70 and that which began in 1995 (Fig. 4.22c). NOAA’s detrended Kaplan AMO index for ASO 2016 was $+0.44$ (see report Appendix for link) and has been positive for the ASO season since 1995 (Bell et al. 2016).

The Atlantic warm pool (AWP) reflects the area of SSTs greater than 28.5°C (Wang 2015). The AWP during ASO 2016 extended eastward across the entire southern MDR (black contour; Fig. 4.22a), which far exceeds its climatological extension to the central MDR (brown contour). The AWP during ASO 2016 also extended farther north than normal over the western North Atlantic. As a result, the average size

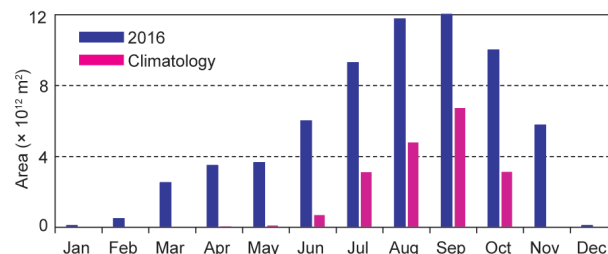


FIG. 4.23. Monthly size of the Atlantic warm pool (AWP) in 2016 (10^{12} m^2 ; blue) and the climatological AWP area (red). Climatology is the 1971–2000 ERSST-v4 (Huang et al. 2015) mean area of the 28.5°C SST isotherm.

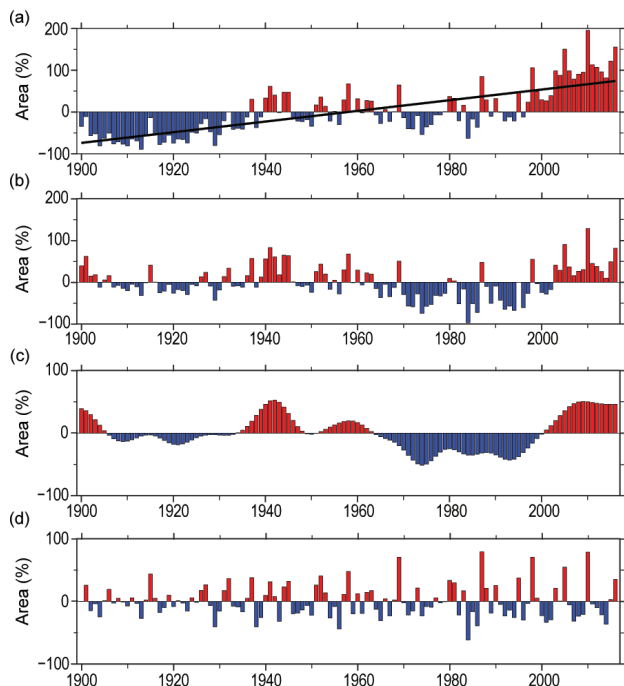


FIG. 4.24. AWP index (%) for 1900–2016, calculated as the anomalous area of SST warmer than 28.5°C during Jun–Nov divided by the climatological AWP area. Shown are the (a) total, with linear trend indicated (black line), (b) detrended (removing the linear trend), (c) multidecadal, and (d) interannual area anomalies. The multidecadal variability is obtained by performing a seven-year running mean to the detrended AWP index. The interannual variability is calculated by subtracting the multidecadal variability from the detrended AWP index. [Source: ERSST-v4 (Huang et al. 2015) dataset.]

of the AWP during ASO 2016 was more than double its climatological mean (Fig. 4.23).

The 2016 AWP was bigger and lasted longer than the climatological mean throughout nearly the entire year. It persisted for 10 months during 2016 (February through November), while the climatological mean warm pool is present for just five months (June–October). By July, the 2016 warm pool had already exceeded its September climatological peak.

The description and characteristics of the AWP, including its multidecadal variability, have been previously described (Wang 2015). Figure 4.24 shows the extension of the annual AWP time series through 2016, along with its variability on different time scales. Overall, the time series shows an upward trend since 1900 (Fig. 4.24a), along with significant multidecadal and interannual variability (Figs. 4.24b–d). Its multidecadal fluctuations coincide with those of the AMO (Fig. 4.24c). The transition to an anomalously large size of the AWP in 1995 coincided with

a transition to the warm phase of the AMO (e.g., Bell et al. 2016).

(iv) Atmospheric conditions

The atmospheric circulation during ASO featured an extensive and persistent ridge of high pressure in the middle and upper troposphere over the western half of the subtropical and tropical North Atlantic Ocean and Caribbean Sea (Fig. 4.25a). Within the MDR, the southern flank of this ridge featured anomalous upper-level easterly winds (see Fig. 4.6c) and anomalous lower-level westerly winds (see Figs. 4.5c,d). The ridge was also associated with a northward shift of the extratropical westerly winds along its northern flank. This wind pattern contributed to an extensive area of weak vertical shear across the western half of the Atlantic basin and the southeastern United States (shading, Fig. 4.25a), with anomalously weak shear spanning the central MDR and the eastern half of the United States (Fig. 4.25b). On monthly time scales, shear values less than 8–10 m s⁻¹ are generally considered conducive to hurricane formation (Gray 1968; DeMaria et al. 2005; Tippett et al. 2011).

The anomalous ridge was also associated with enhanced midlevel moisture and anomalous upper-level divergence over the western subtropical North Atlantic (Fig. 4.26). At 600 hPa, area-averaged moisture in that region during ASO was the third largest in the 1970–2016 record (Fig. 4.26a). The area-averaged anomalous divergence during September–October was the largest since the record-breaking Atlantic hurricane season of 2005 (Fig. 4.26b).

All of the above conditions were main contributors to the increased strength of the 2016 Atlantic hurricane season compared to the past three seasons and also to the increased activity over the Caribbean Sea. Those conditions also allowed more storms to track farther westward, increasing the number of landfalls in both the United States and the region around the Caribbean Sea. For example, they were especially prominent during the lifecycle of major Hurricane Matthew, which developed in late September while tracking westward over record-warm waters of the Caribbean Sea (Fig. 4.22d) and then spent its entire life-cycle beneath the upper-level ridge while making landfall in several nations.

The conditions over the western half of the Atlantic basin during ASO 2016 differ notably from the climatological mean. Normally, a tropical upper tropospheric trough (TUTT) is present over the western subtropical North Atlantic and extends southward into the western and central MDR. An enhanced TUTT, along with its associated patterns of strong

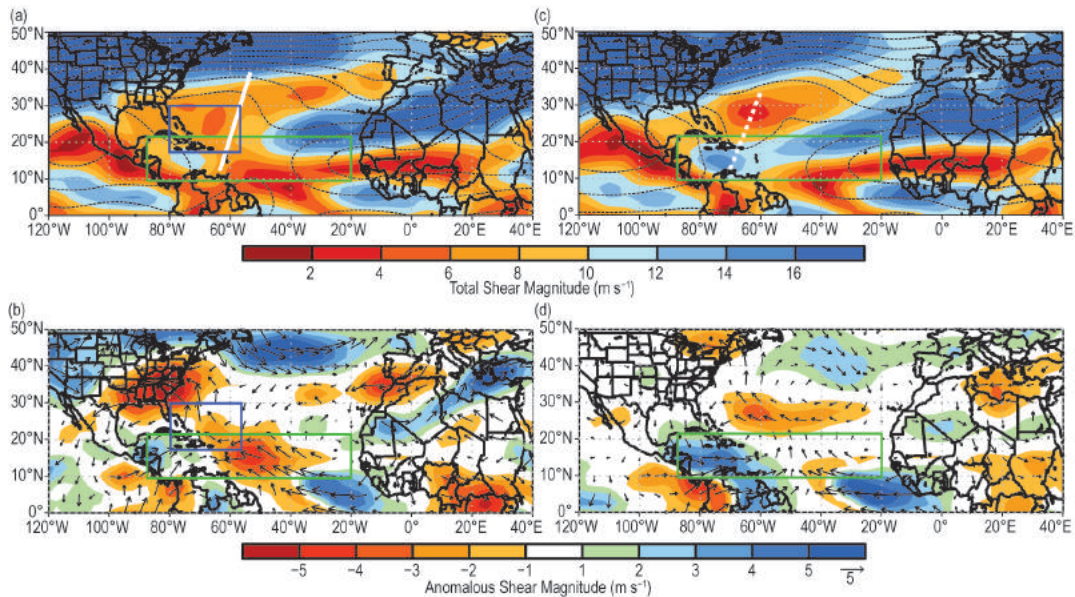


FIG. 4.25. NCEP-NCAR reanalysis (Kistler et al. 2001) 200–850-hPa vertical wind shear (a),(c) magnitude (shaded, m s^{-1}) and (b),(d) anomalous magnitude and vector. (a),(b) ASO 2016 conditions and (c),(d) ASO 2013–15 averages. In (a),(c), the 200-hPa streamfunction field is overlaid (contours; interval: $5 \times 10^6 \text{ m}^2 \text{ s}^{-1}$), the upper-level ridge and TUTT discussed in the text are labeled, and orange-red shading indicates areas where the vertical wind shear magnitude is $\leq 10 \text{ m s}^{-1}$. In (b),(d) anomalous shear vector scale is below right of color bar. Blue box in (a),(b) shows the averaging region for Fig. 4.26. Green boxes denote the MDR. Anomalies are departures from 1981–2010 means.

vertical wind shear (Figs. 4.25c,d), anomalously dry air, and anomalous sinking motion across the Caribbean Sea, was an important contributor to the reduced hurricane activity observed during 2013–15 (Bell et al. 2014, 2015, 2016).

During October and November, the upper-level ridge over the western part of the basin was linked to La Niña, whose larger-scale circulation pattern extended across the entire subtropical Pacific Ocean in both hemispheres (Fig. 4.27a). As indicated in

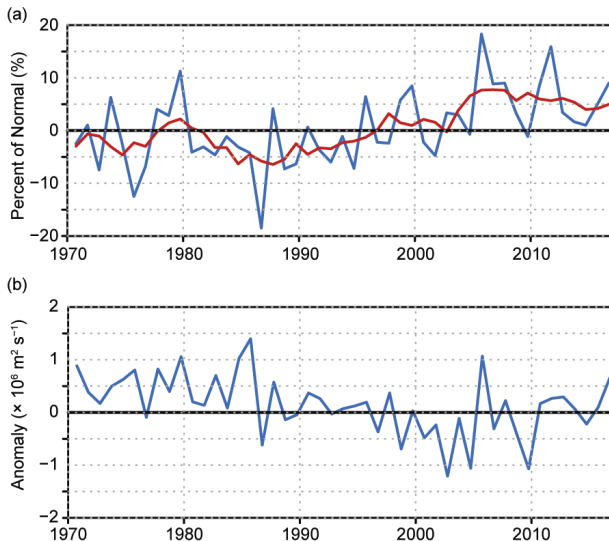


FIG. 4.26. NCEP-NCAR reanalysis (Kistler et al. 2001) time series for 1970–2016 showing (a) ASO percent of normal area-averaged specific humidity and (b) Sep–Oct area-average 200-hPa divergence anomalies ($\times 10^6 \text{ m}^2 \text{ s}^{-1}$). Area averages are calculated for the blue boxed region ($57.5^{\circ}\text{--}80^{\circ}\text{W}$ and $17.5^{\circ}\text{--}30^{\circ}\text{N}$) in Fig. 4.25a. Anomalies are departures from 1981–2010 means.

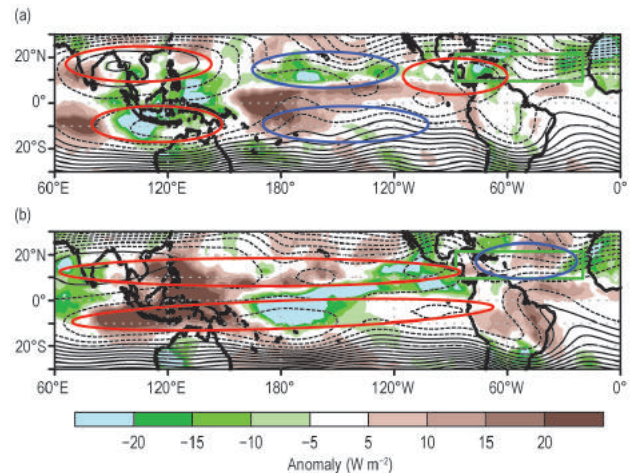


FIG. 4.27. 200-hPa streamfunction (contours; interval: $5 \times 10^6 \text{ m}^2 \text{ s}^{-1}$) from the NCEP-NCAR reanalysis (Kistler et al. 2001) and anomalous OLR (shaded, W m^{-2} ; Liebmann and Smith 1996) during (a) Oct–Nov 2016 and (b) Oct–Nov 2015. Ridges (red ovals) and troughs (blue ovals) discussed in the text are indicated. In the tropics, green (brown) shading indicates enhanced (suppressed) convection. Anomalies are based on the 1981–2010 climatology.

the 200-hPa streamfunction field, that typical La Niña pattern featured a westward retraction of the mean subtropical ridges over the western Pacific (coinciding with enhanced equatorial convection), amplified mid-Pacific troughs in both hemispheres (coinciding with suppressed equatorial convection), and a pronounced downstream ridge extending across the Caribbean Sea. This wave pattern is notably different from the typical El Niño-related pattern observed during October–November 2015 (Fig. 4.27b), which suppressed Atlantic hurricane activity—that pattern featured extended subtropical ridges across nearly the entire Pacific basin in both hemispheres and an extensive downstream trough across the entire MDR.

3) EASTERN NORTH PACIFIC AND CENTRAL NORTH PACIFIC BASINS—M. C. Kruk and C. J. Schreck

(i) Seasonal activity

The eastern North Pacific (ENP) basin is officially split into two separate regions for the issuance of warnings and advisories by NOAA’s National

Weather Service. NOAA’s National Hurricane Center in Miami, Florida, is responsible for issuing warnings in the eastern part of the basin (ENP) that extends from the Pacific Coast of North America to 140°W, while NOAA’s Central Pacific Hurricane Center in Honolulu, Hawaii, is responsible for issuing warnings in the central North Pacific (CNP) region between 140°W and the date line. This section summarizes the TC activity in both warning areas using combined statistics, along with information specifically addressing the observed activity and impacts in the CNP region.

The ENP/CNP hurricane season officially spans from 15 May to 30 November. Hurricane and tropical storm activity in the eastern area of the basin typically peaks in September, while in the CNP TC activity normally reaches its seasonal peak in August (Blake et al. 2009). During the 2016 season, a total of 21 named storms formed in the combined ENP/CNP basin (Fig. 4.28a). This total includes 12 hurricanes, 5 of which were major hurricanes. The 1981–2010 IBTrACS seasonal averages for the basin are 16.5 named storms, 8.5 hurricanes, and 4.0 major hurricanes (Schreck et al. 2014).

The 2016 seasonal ACE index was $188.7 \times 10^4 \text{ kt}^2$ (Fig. 4.28b), which is above the 1981–2010 mean of $132.0 \times 10^4 \text{ kt}^2$ (Bell et al. 2000; Bell and Chelliah 2006; Schreck et al. 2014). By comparison to the 2015 season, which featured a record-shattering 16 tropical cyclones in the CNP basin, the 2016 season featured only 6 storms. Nonetheless, 2016 was still above the long-term 1981–2010 IBTrACS mean of 4.7 storms passing through the CNP per season.

(ii) Environmental influences on the 2016 season

Figure 4.29 illustrates the background conditions for TC activity in the ENP and CNP during the 2016 season. Consistent with the moderate La Niña conditions later in the season, the equatorial Pacific was dominated by anomalously cool SST anomalies (Fig. 4.29a). As in recent years, however, anomalously warm SSTs prevailed farther north. The ITCZ was also enhanced and shifted somewhat northward (see Section 4d) in association with the SST pattern with most of the TCs forming on the eastern end of that enhanced convection (Fig. 4.29b). Wind direction anomalies were generally westerly, but the vertical wind shear magnitudes were still slightly below their climatological values (Fig. 4.29c). The other years within this recent active period (2012–15) all featured broad areas of 850-hPa westerly anomalies (Diamond 2013, 2014, 2015; Diamond and Schreck 2016). In this respect, 2016 is an outlier (Fig. 4.29d).

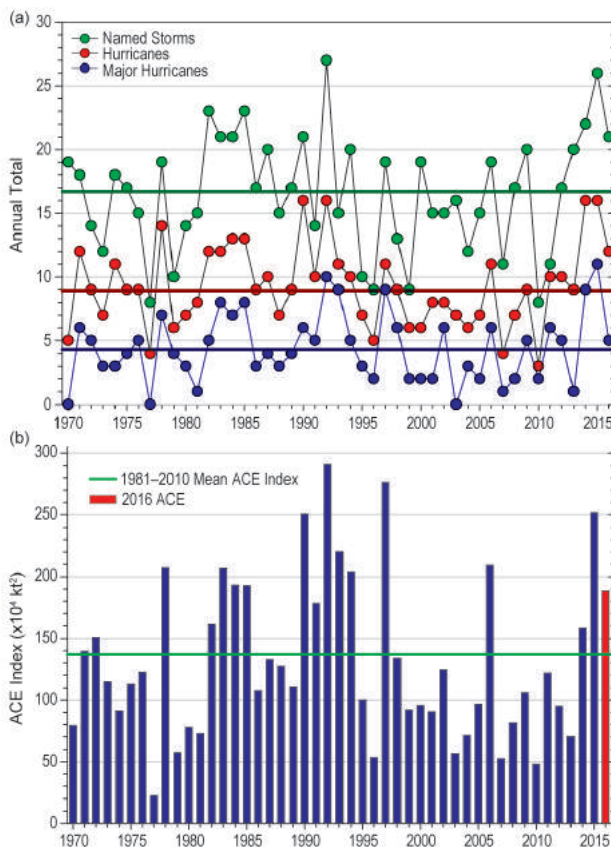


FIG. 4.28. Seasonal TC statistics for the full ENP/CNP basin over the period 1970–2016: (a) number of named storms, hurricanes, and major hurricanes, and (b) the ACE index ($\times 10^4 \text{ kt}^2$) with the 2016 seasonal total highlighted in red. Horizontal lines denote the corresponding 1981–2010 means for each parameter.